

UCRL-JC-131507

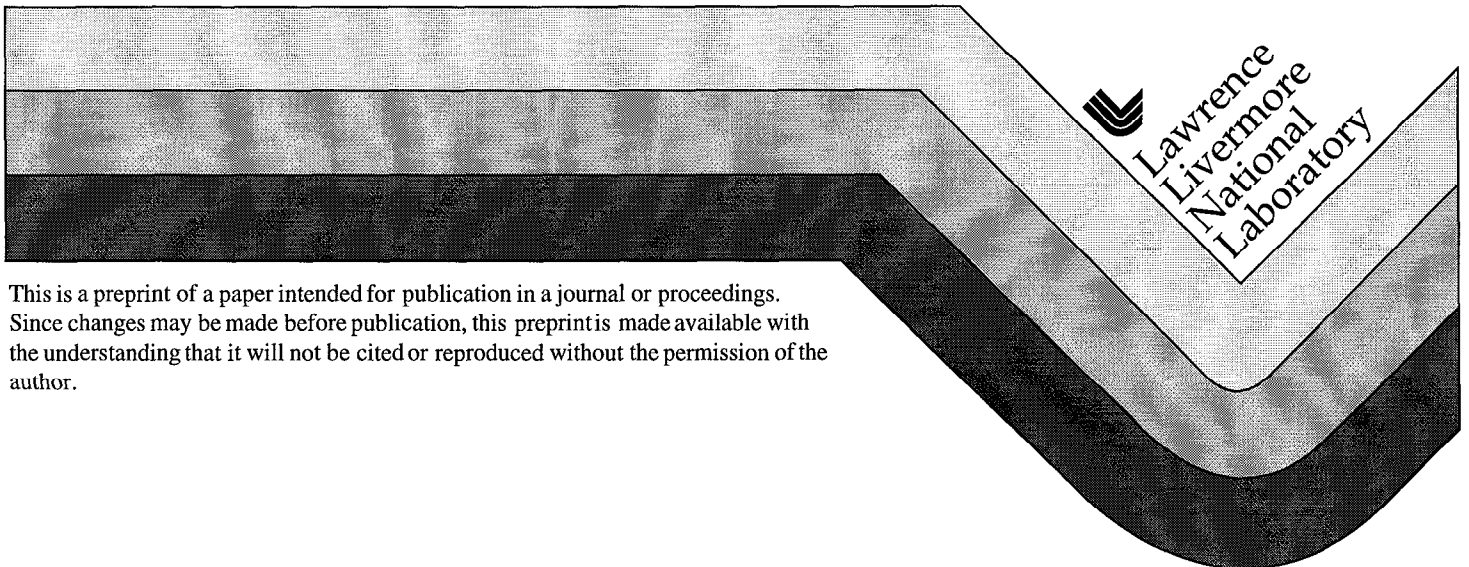
PREPRINT

Use of Alternating-Z Doubling in High-Dynamic-Range Tripling: Design and Evaluation of an Optimized Prototype Tripler

D. Milam
D. Eimerl
J. M. Auerbach
C. Barker
P. W. Milonni

This paper was prepared for submittal to the
Third Annual International Conference on
Solid State Lasers for Application (SSLA)
to Inertial Confinement Fusion (ICF)
Monterey, California
June 7-12, 1998

July 27, 1998



This is a preprint of a paper intended for publication in a journal or proceedings.
Since changes may be made before publication, this preprint is made available with
the understanding that it will not be cited or reproduced without the permission of the
author.

DISCLAIMER

This document was prepared as an account of work sponsored by an agency of the United States Government. Neither the United States Government nor the University of California nor any of their employees, makes any warranty, express or implied, or assumes any legal liability or responsibility for the accuracy, completeness, or usefulness of any information, apparatus, product, or process disclosed, or represents that its use would not infringe privately owned rights. Reference herein to any specific commercial product, process, or service by trade name, trademark, manufacturer, or otherwise, does not necessarily constitute or imply its endorsement, recommendation, or favoring by the United States Government or the University of California. The views and opinions of authors expressed herein do not necessarily state or reflect those of the United States Government or the University of California, and shall not be used for advertising or product endorsement purposes.

Use of Alternating-Z Doubling in High-Dynamic-Range Tripling: Design and Evaluation of an Optimized Prototype Tripler

D. Milam, D. Eimerl, J. M. Auerbach, and C. Barker

Lawrence Livermore National Laboratory

P. W. Milonni

Los Alamos National Laboratory

Abstract

We designed and tested an alternating-Z tripler that consisted of two detuned, Type-I, potassium dihydrogen phosphate (KD*P) doublers and one KD*P mixer. The crystal thicknesses were, respectively, 13, 10 and 10 mm, and the detunings of the doublers were +420 and -520 μ rad. All three crystals were fabricated from 80% deuterated KDP. Conversion efficiency was measured and calculated for input 1053-nm pulses with approximately rectangular waveforms and durations of either 1 or 6 ns, and for 20-ns pulses that exhibited intensity variation by a factor of 10. The measured peak conversion efficiency was more than 80%, and energy conversion efficiencies ranged from 62-80% depending on the waveform of the input pulse. The expected large dynamic range in input intensity, 9-10, was observed, and the measured and calculated efficiencies were in excellent agreement.

I. Introduction.

Since its discovery 37 years ago[1], harmonic conversion has evolved to a stage that allows production in fusion laser facilities of 351-nm pulses with energy of tens of kilojoules[2-6]. The standard two-crystal configuration [7] for frequency tripling of 1053-nm, short-duration pulses uses one crystal as a doubler and a second as a mixer. For a selected range of input intensities, the tripling efficiency of a two-crystal converter can exceed 80% [8].

The dynamic range Ω of a convertor is defined to be the ratio of the highest and the lowest input intensities that provide a specified conversion efficiency. In

This work was performed under the auspices of the U.S. DOE by LLNL under contract No. W-7405-Eng-48.

the two-crystal tripler, the dynamic range is largely determined by the doubler. One approach to increasing the dynamic range, usage of multiple crystals, was first conceived more than 30 years ago. The stack-of-plates design [9,10] was proposed as a technique for obtaining quasi-phase matching over a relatively long path in an isotropic material, and demonstrated in GaAs [11,12], CdTe [13], and SiO₂ [14]. A key element in these designs was the alternating-Z arrangement. One out of every pair of crystals in the stack was flipped so that the orientation of the C axis in one crystal was opposite that in the preceding crystal. Phase mismatch that accumulated in one crystal was canceled in the next.

For birefringent materials, multiple passage of the beam through one crystal during intracavity doubling of YAG lasers [15] was the first significant application of the multiple-crystal harmonic conversion. Later, Volosov et al studied doubling in two KDP crystals that were used in tandem in a beam that was external to a laser cavity [16]. They experimentally and theoretically evaluated the four possible arrangements of two Type I doublers in series, and the two arrangements of Type II doublers. The combination that is now known as the Type I alternating-Z was least sensitive to beam divergence, and most successful at preventing back conversion.

Eimerl provided a thorough analysis of N-plate, alternating-Z doublers, which could be cooled by flowing gas between the plates. His work indicated that these devices could provide high efficiency at low to moderate input power, and that they could tolerate the large thermal loading in a high-average-power laser[17]. KD*P doublers were built according to the principles of that analysis, and used with a slab-glass laser [18,19]. An alternating-Z doubler with two 2.5-cm-thick KD*P crystals generated more than 100 W of second-harmonic (527-nm) light, in a nearly diffraction limited beam, at a relatively low 1053-nm input intensity of 100-200 MW/cm² [18]. With an improved slab laser and a similar doubler, conversion efficiency of 80% was obtained at 185 MW/cm², and at a total output power of more than 100 W at 527-nm[19].

Usage of more than two KD*P crystals for doubling was reported by Siebert et al[20]. Their 3-crystal doubler provided efficiency of 28% while converting long-

duration pulses at input powers below 85 MW/cm². Addition of a 4-crystal mixer yielded third-harmonic conversion efficiency of 21%.

Finally, the quadrature arrangement uses two doublers that are in tandem but not arranged in the alternating-Z configuration[21]. One doubler is rotated about the beam by 90° relative to the other, and the output is two second-harmonic waves that are orthogonally polarized. A demonstration device was assembled from bare, 91% deuterated KD*P[21]. It had one 12-mm-thick doubler that optimally converted at high input intensity and one 44-mm-thick doubler for conversion at low intensity. It achieved 80% efficiency for input intensities between 1 and 6 GW/cm², even though the reflective and absorptive losses were estimated to be 15-18%. Pronko et al. extended the analysis of quadrature doubling to include the case of broadband input pulses [22]. They demonstrated efficiency of 55% for a KDP quadrature doubler with input pulses that had intensities as large as 1 GW/cm², energies to 500 J, and bandwidth of 17 cm⁻¹.

Recent calculations [23] indicated the merit of three- and four-crystal triplers for conversion of the high-fluence pulses that will be produced by the National Ignition Facility (NIF) laser[24]. KDP crystals with aperture of 40 cm will be used to triple 1053-nm pulses with durations ranging from 1-20 ns. Output intensities at 351 nm will range from 0.05 GW/cm² in segments of the 20-ns pulse to 5 GW/cm² in short pulses. Efficient conversion over a wide intensities is a logical application of the alternating-Z arrangement. Such a tripler has been optimized, built, and tested. This paper describes the optimization procedure, provides graphs that illustrate the calculated performance of the optimized tripler, and describes the results of several conversion experiments. In an appendix, we provide a discussion of dispersion in the air gap between the doublers in an alternating-Z tripler.

II. Optimization of a High-Dynamic-Range Alternating-Z Tripler.

The basic idea of the alternating-Z approach is that the phase mismatch developed in the first crystal is compensated in the second crystal, and one of the basic ideas of multiple-crystal schemes is that crystals with different lengths perform most efficiently in different intensity ranges. Therefore, we would expect that the alternating-Z doubler would have two crystals with different lengths, each with an

angular offset to provide the correct mix ratio, and that the angular offsets would be such that the dephasing accumulated in the first would be compensated in the second. These requirements suggest that the ratio of the detuning angles should be the inverse of the ratio of the crystal lengths, and that the detunings should be of opposite sign.

This elementary picture, and detailed calculations that were done with Runge-Kutta codes, were used to optimize the alternating-Z design for frequency tripling in the NIF.

Several almost equivalent designs were found. The doublers can be either Type I or Type II, and the orientation of the doublers can be either tandem or alternating-Z. We selected Type I doublers, because they could be cut from a smaller boule, but used a Type II mixer. This design was optimized under three assumptions, (1) that the divergence of the input beam was $50 \mu\text{rad}$, (2) that most of the beam energy was delivered at intensities between 0.1 and 5 GW/cm^2 , and (3) that the length of the air gap between the doublers could be adjusted so that air-gap dispersion had no effect on conversion efficiency. Table I contains a summary of the optimized design.

We adopt the designation AZ- D_1 - D_2 - D_3 - φ for an alternating-Z tripler. D_1 and D_2 are thicknesses of the doublers, the D_3 is the thickness of the mixer. φ is the phase shift of the 527-nm wave relative to the 1053-nm wave, after these waves have propagated through the air gap between the doublers.

III. Example Calculations for the alternating-Z tripler.

This section contains graphs that were selected to demonstrate the characteristics of an alternating-Z tripler, and to allow them to be compared with the properties of a two-crystal TypeI/TypeII tripler. All of the example calculations were done with a plane-wave code, after the completion of optimization and experimental studies. Hind sight assisted in selection of relevant examples, and some experimental data were used in the calculations. For example, we assumed that the optical surfaces of the crystals were coated with a silica sol-jel anti-reflective

layer, and used values of single-surface transmittance that were measured for the crystals in a prototype AZ-13-10-10 convertor (see Table 2 below).

Figure 1 contains optimized conversion curves for AZ-13-10-10- 2π and AZ-13-10-13- 2π triplers made of 80% deuterated KDP. For both calculations, angular offsets of the 13- and 10-mm doublers were, respectively, 400 and -520 μrad (internal), and dispersion in the air gap was ignored ($\varphi = 2\pi$). Varying the thickness of the mixer changes the intensity band, but it does not significantly alter the dynamic range. The dynamic range at 60% conversion is 9 for the AZ-13-10-13- 2π tripler, and 10 for the AZ-13-10-10- 2π tripler. Figure 1 also contains the conversion curve for an 80% deuterated two-crystal Type I/ Type II convertor with an 11-mm doubler and a 9-mm mixer. The peak efficiency is larger, primarily because there are fewer surfaces, but the dynamic range of the two-crystal convertor at 60% conversion is 6.

Figure 2 illustrates the effect of air-gap dispersion on conversion by an AZ-13-10-10 tripler with doubler offsets of +425 and -520. The listed phase errors, 0.15 and 0.20 radians, are departures from the desired value of 2π . These small phase errors cause a large reduction in efficiency at high efficiency. The associated errors in the length of the air gap, about 3.1 and 4.2 mm, are large relative to the tuning capabilities of even simple mechanical devices. The phase error could, in principle, easily be eliminated.

One of the most interesting differences between alternating-Z and the two-crystal triplers is that greatest efficiency over the entire design range of intensities is obtained for one unique set of detunings for the alternating-Z doublers, whereas the intensity band can be shifted by retuning the doubler in the two-crystal tripler. For small variations from optimum detunings, the efficiency of the alternating-Z tripler is effected only at the largest intensities in the design band, see Fig. 3. The effect of severe departure from the optimum detuning is illustrated in Fig. 4. For the calculations in Fig. 4, the offset of the 13-mm doubler was held at 400 μrad , and the offset of the 10-mm doubler was varied in steps from 0 to -520 μrad .

IV. Experimental Arrangement and Measurements.

We assembled an AZ-13-10-10 tripler and tested it in the arrangement that is shown in Fig. 5. The input 1053-nm beam was shaped by apodization and image relaying, and it was 22 mm in diameter. The fluence distribution in the beam, the temporal waveform and the pulse energy were measured for each input pulse. A typical input fluence distribution is shown in Fig. 6. The intensity modulation consisted of diffraction rings that were a residual of the beam apodization, and random structure that was caused by imperfections in optical components within the chain. An aperture with diameter of 13 mm was placed in the path to the calorimeter. Input fluence was calculated as the spatial average over this aperture. Calculated transmittance and reflection coefficients of the silica splitter were used to relate fluence in the calorimeter arm to that in primary beam in the input plane to the crystals. Use of apertured calorimetry was done to avoid the necessity of modeling the conversion of the varied intensities in the shoulders of the spatial distribution.

The output diagnostic package is also shown in Fig. 5. A sample of the three-frequency output beam was reflected by the front surface of a bare silica wedge, and passed through an aperture with diameter of 13 mm. The apertured beam was dispersed by two silica prisms, and the energy and fluence distribution were measured for each of the harmonics. Spatially averaged output fluences were calculated from the area of the aperture and the energies.

The arrangement of the crystals is shown in Fig. 7. They were fabricated of 80% deuterated material by diamond turning, and had aperture of 50 x 50 mm. Each crystal was housed in a thermal enclosure and maintained at a temperature of 24.2 ± 0.1 °C, which was about 2 degrees above room temperature. Each oven was mounted in a gimbal that allowed angular tuning, and on a precision translation stage that allowed motion of the oven and crystal in and out of the beam. The separation of the interior faces of the two doublers was 13.1 cm.

Surfaces of the crystals were coated with single-layer silica sol-gel antireflection coatings. The intent was to coat the input surface of the first doubler for best transmittance at 1053 nm, and the output surface of the mixer for best transmittance

at 351-nm. Each of the 4 interior surfaces received a coating that was designed to simultaneously optimize transmittance at 1053 and 351 nm. Table 2 contains measured values of surface transmittance. Except for the 351-nm transmittance at the output surface, all of these transmittances agree with calculated values.

The doublers were translated into the beam one at a time and independently oriented by rocking curves generated at intensities of about 3 GW/cm². The tripler was rocked at input intensity of about 2 GW/cm² while one of the aligned doublers was in the beam. The gimbals were used to set the detunings (internal) of +420 μ rad for the 13-mm doubler and -520 μ rad for the 10-mm doubler. The uncertainty of the angular alignment has three components, the pointing stability of the laser (± 10 μ rad), the precision of the curve fit to the rocking data (± 10 μ rad), and the accuracy of the detuning by the gimbal (± 5 μ rad). Under the assumption that these are independent, the alignments should have been accurate to within ± 15 μ rad during a typical shot.

We studied conversion of input 1053-nm pulses with duration of 1, 6 and 18 ns that were shaped by a serial arrangement of 3 Pockels cells. The 1-ns pulses were used to measure the 527-nm to 1053-nm mix ratio for the two-crystal doubler, and the 351-nm conversion efficiency for the tripler. Use of the 1-ns pulses allowed testing at input intensities above 5 GW/cm² without threat of laser-induced damage. The 6-ns pulses were used to study conversion at low input intensity because fluence measurements at low intensity were more accurate for these longer pulses. To demonstrate the large dynamic range of the alternating-Z tripler, we used an 18-ns pulse which had a intense 2-ns segment. Waveforms of the input 1053-nm pulses were recorded by a Hamamatsu photodiode and a Tektronix SCD5000 digitizer. Typical input 1053-nm waveforms are shown in Fig. 8. During some of the experiments, the waveform of the 351-nm pulse was recorded by a streak camera; examples will be shown below.

V. Data and analysis.

The data were modeled by the plane-wave code that had been used during the design optimization. The code was used to generate a look-up table that gave conversion efficiency as a function of input intensity. For each shot, the waveform of the input 1053-nm pulse was calibrated (in Watts/cm²) to agree with the measured input fluence, and the look-up table was used to predict the corresponding 351-nm waveform. Fluence at 351 nm was calculated by integrating the waveform. This shot-by shot process was selected because there were small variations in the recorded 1053-nm waveforms. To determine the significance of these variations, we also modeled all of the data in each set using one representative 103-nm waveform.

Figure 9 shows the mix ratios that were measured for the doubler with 1-ns pulses, and the results from two models of the data. The measured mix ratio rose rather slowly with increase in input intensity, and had a positive slope when it passed through the optimum value of 2:1. Modeling indicates that the slow rise was caused by the variation of intensity during the rise time (about 0.2 ns) of the 1-ns pulses. Our attempts to understand why the mix ratio was greater than 2:1 at high intensity led to the necessity of invoking air-gap dispersion. We initially assumed that the high mix ratio was a result of experimental errors in the detunings of the doublers, but found that this assumption required errors that were about 4 times larger than the likely uncertainty of 15 μ rad. We found that the high value of the mix ratio could be explained by assuming a small phase shift, -0.15 radians, for the 527-nm wave.

Figure 10 shows the tripling efficiencies that were measured with 6-ns low-intensity pulses, efficiencies that were calculated by applying the look-up table to the measured 6-ns 1053-nm waveforms, and a curve that is a plane-wave calculation (assumption of precisely rectangular input waveforms). The close agreement between measurements and modeling for this low-intensity data provides confirmation that the code contained reasonable values of coupling coefficients and transmittances. At low-intensity, conversion efficiency depends strongly on those

parameters, whereas it is not strongly effected by either small errors in the tuning of the crystals or a small air-gap dispersion.

Conversion efficiencies that were measured with relatively intense 1-ns pulses are shown in Fig. 11. For an input pulse with peak intensity of about 3 GW/cm², the energy efficiency was 75% and the peak efficiency was 80%. Peak conversion of 83% was predicted by the code for rectangular pulses. For intensities larger than 4.5 GW/cm², the measured values were systematically less than those calculated from measured waveforms.

While the parameter of principal interest was the third-harmonic efficiency, the output fluences for all three harmonics were calculated and measured. Figure 12 shows these results for the 1-ns experiment. The solid curves are simply visual aids that were fitted through all of the data, either calculated or measured, for each harmonic. The agreement between calculated and measured values of the residual 527-nm and 1053-nm fluences is acceptable because the uncertainty in calorimetry increases as the input fluence decreases.

The final experiment was conversion of the temporarily shaped 18-ns pulses. An example is shown in Fig. 13. The figure contains measured waveforms for the input 1053-nm pulse and the output 351-nm pulse, each calibrated to agree with the relevant measured fluence, and a 351-nm waveform that was calculated via the look-up table from the 1053-nm pulse

The measured and calculated 351-nm waveforms are in close agreement. The difference was greatest during the rise of the intense segment. Some of that difference was caused by the presence a small dip in the calibrated 1053-nm waveform. The harmonic-conversion look-up table transferred the dip to the calculated 351-nm waveform. A corresponding dip was not observed in the measured 351-nm waveform. We suspect, therefore, that electronic noise accounts for the 1053-nm transient.

Table 3 provides the peak and energy efficiencies and the peak-to-foot, 351-nm intensity ratios for two of the 18-ns experiments. The peak-to-foot ratio is the intensity in the 2-ns segment, divided by average of the intensity in the flattest portion in the leading wing of the foot. The code accurately predicted the measured

peak and energy efficiencies. The calculated 351-nm peak-to-foot ratios are smaller than the measured ratios, but a relatively large experimental uncertainty is expected in the measurement of such large ratios.

VI. Creation of a NIF Baseline 351-nm Pulse.

One of the design goals for NIF is the generation of 21-ns, 351-nm pulses that exhibit 50:1 temporal variation of intensity and peak intensity of about 2.5-3.0 GW/cm². The waveform of this 351-nm NIF pulse was specified; the waveform of the required input 1053-nm pulse will be dictated by the conversion efficiency. The required 1053-nm pulse was calculated for four triplers made of 80% deuterated KDP; (AZ-13-10-10-0.15 radians), (AZ-13-10-10-2 π), (AZ-13-10-13-2 π), and the two-crystal Type I/Type II 11mm-9mm design. All of the calculations were done using look-up tables that were created during modeling of the data or calculation of examples, with due care exercised to properly treat the double-valued functions that result when the tables are used to calculate the 1053-nm waveform.

Figure 14 shows the NIF 21-ns 351-nm pulse, and the input 1053-nm pulses that were calculated for two triplers, the (AZ-13-10-13, 0 radians) and the two-crystal design. The predicted 1053-nm waveforms for the other two alternating-Z triplers were similar in appearance. Table 4 provides four parameters that characterize the triplers; the peak and foot intensities of the required 1053-nm pulse, and the peak and energy conversion efficiencies. The energy efficiency is predicted to be largest, 68%, for the AZ-13-10-13 tripler. The improvement is solely due to the better conversion efficiency at low intensity. That allows reduction foot intensity from 0.334 GW/cm² for the 11-9 tripler to 0.204 GW/cm² for the alternating-Z tripler.

VII. Summary:

We presented calculations that describe the principal characteristics of an alternating-Z tripler which consists of two detuned Type I doublers and one aligned Type II mixer. The calculations predict that the pair of doublers in the Alternating-Z arrangement can hold the mix ratio at or near the optimum value of 2:1 for a wide range of input 1053-nm intensities. This insensitivity to variation in input intensity, or large dynamic range, makes the Alternating-Z interesting for

applications where there are large excursions of intensity in either the waveform or the spatial distribution of the laser pulse.

An alternating-Z tripler that had doublers with thicknesses of 13 and 10 mm, and a 10-mm-thick mixer was tested. All of the crystals were 80% deuterated. The mix ratio for the doublers was measured with 1-ns 1053-nm pulses. The 351-nm conversion efficiency was measured for 1- and 6-ns rectangular pulses, and for 20-ns pulses with a 12:1 temporal variation of intensity.

The majority of the experimental results were accurately described by the model for the Alternating-Z tripler, although it was necessary to assume that dispersion in the air gap between the doublers had caused a phase lag of 0.15 radians for the 527-nm wave. The agreement between the theory and the experimental results confirmed the prediction of large dynamic range.

We also considered the problem of generating the 21-ns 351-nm baseline pulse for the NIF laser. The waveform for this 351-nm pulse has a specified shape that contains a 50:1 variation of intensity. An energy efficiency of 62% was calculated for the AZ-13-10-10 tripler, using the model that assumed an air-gap phase error. Because the triplers for NIF will be installed in vacuum, it is presumed that the phase errors will be eliminated. Then the predicted energy efficiencies are 65% for an AZ-13-10-10 tripler and 68% for an AZ-13-10-13 tripler. For the 2-crystal Type I/Type II triplers with 80% deuterated crystals, the predicted efficiency is about 55%.

VIII. Acknowledgments.

The experimental study was done in the Optical Sciences Facility at Lawrence Livermore Laboratory. We are grateful for the assistance of Walter Sell, who maintained and operated the laser in this facility, and collected most of the data during the conversion experiment.

Appendix. Dispersion in an Air Gap Between Two Doublers.

When two doublers are used in any tandem arrangement except quadrature, the net second-harmonic wave is a sum of two independently generated fields, one from each of the crystals. Correct functioning of the doubler requires constructive, in-phase addition of these two fields.

Dispersion in the air gap between the two crystals can impair this summation.

Passage of the fundamental field through either of the doublers creates a second-harmonic wave that is phase locked to the fundamental. This phase-locking should be interpreted in terms of an instantaneous picture of the spatial variation of the electric fields of the fundamental and second-harmonic waves. Such a picture would show that in any cycle of the fundamental wave there are two cycles of the second-harmonic wave, that is two crests and valleys, and that the crests of the second harmonic coincide with the zeros of the fundamental. Dispersion in the air gap can cause a relative phase retardation of the second-harmonic wave from the first crystal, and prevent its in-phase addition to the second-harmonic wave in the second crystal.

The difficulties that arise though air-gap dispersion were recognized in some of the earliest studies of harmonic conversion. The first experimental treatment occurred during optimization of oscillators with internal second-harmonic conversion[15]. The converter crystal was placed in one end of the cavity, near a mirror that was shared by both the 1064- and 532-nm beams, and the spacing of the mirror and the crystal was adjusted to provide maximum conversion. The optimum air path, 13.1 cm, was assumed to be that necessary for a 2π relative phase retardation of the second-harmonic. It was in reasonable agreement with the value of 12.4 cm that was calculated[15] from the dispersion data of Miller[25]. Dmitriev et al[26] also used a folded path that contained a mirror to study the effect of dispersion on two-pass conversion efficiency for doublers that were either inside or outside a laser cavity. Their experimental value for the 2π spacing was 10-12 cm, and they used index data of Kay and Laby [27] to calculate a spacing of 13 cm. In both experiments [15,26], some fraction of the dispersion might have arisen in the folding mirror.

There are three additional measurements of the air gap dispersion[16,28,29]. Volosov et al.[16] and Summers and Boyd[28] passed a beam through two separate doublers and measured the efficiency as a function of crystal separation. The measured 2π values were, respectively, 13.0 and 15.0 cm. Velsco and Eimerl [29]

installed a gas cell between two crystals and measured conversion efficiency as a function pressure in several gases. For dry air at atmospheric pressure and at 24 °C, they found that a 2π phase shift occurred for a change in crystal separation of 13.09 cm.

Finally, it is somewhat coincidental that conversion was optimized in most of these early studies by a phase shift of 2π , since the correct phase shift is partially dictated by the orientations of the crystalline axes in the doublers. For doubling, the important nonlinear parameter is d_{eff} . The sign of this coefficient varies with Z-axis orientation and with the XY cut of the crystal. KDP has tetragonal symmetry, so that equivalent positions are found by rotating the crystal axes by $\pi/2$ about the Z-axis. The d_{eff} changes sign under this rotation, so that there are two types of crystals. For example, for type I crystals, the input face may contain either a crystalline X-axis, or a Y-axis. (For type II the input face may contain either an (X+Y) or an (X-Y) direction.) These two cuts will perform equally well as single crystal doublers but their d-coefficients have opposite signs.

The relative sign of the d-coefficients can be written

$$\frac{d_1}{d_2} = \xi_{xy} - \xi_Z \quad (2)$$

Here ξ_{xy} is -1 if the crystals have different XY-cuts, and +1 if they are the same. ξ_Z is +1 if the crystal Z-axes are parallel. The standard alternating-Z configuration is obtained from this parallel case by rotating one of the crystals about the beam direction. Then ξ_Z is +1 for the standard alternating-Z configuration also. If either z-axis is exactly reversed from one of these configurations an additional factor of -1 appears for type I crystals, +1 for type II crystals. Thus for same-cut crystals in the alternating-Z configuration the phase shift in the air gap must be 0 or 2π . If one Z-axis is reversed for type I crystals, the phase shift must an odd multiple of π .

Therefore, the issue of dispersion in the air gap appears to be well understood, but the small discrepancies in measured and calculated values are large enough to be of significance for the alternating-Z arrangement

IX. References

1. P. Franken, A. Hill, C. Peters, and G. Weinreich, "Generation of optical harmonics," *Phys. Rev. Lett.* vol. 7, pp. 118-119, 1961.
2. W. Seka, J. M. Soures, S. D. Jacobs, L. D. Lund, and R. S. Craxton, "GDL: A high-power 0.35 mm laser irradiation facility", *IEEE J. Quant. Electron.*, QE-17, pp. 1689-1693, Sept. 1981.
3. I. N. Ross, M. S. White, J. E. Boon, D. Craddock, A. R. Damerell, R. J. Day, A. F. Gibson, P. Gottfeldt, D. J. Nicholas and C. J. Reason, "Vulcan-A versatile high-power glass laser for multiuser experiments," *IEEE J. Quant. Electron.*, QE-17, pp. 1653-1661. Sept. 1981.
4. G. L. Linford, B. C. Johnson, J. S. Hildum, W. E. Martin, K. Synder, R. D. Boyd, W. L. Smith, C. L. Vercimak, D. Eimerl, and J. T. Hunt, "Large-aperture harmonic conversion experiments at Lawrence Livermore national Laboratory," *Appl. Opt.*, vol. 21, 3633-3643, Oct. 1982.
5. P. J. Wegner, M. A. Henesian, D. R. Speck, C. Bibeau, R. B. Erlich, c. W. Lauman, J. K. Lawson, and T. L. Weiland, "Harmonic conversion of large-aperture 105- μ m laser beams for inertial confinement fusion research," *Appl. Opt.* vol. 31, No. 30, pp. 6414-6426, 1992.
6. C. Saureret "La conversion de frequence," *Commissariat a l'Energie Atomique, Centre de Limeil-Valenton, CEA-R-5383, March 1987 (In French with English summry).*
7. R. S. Craxton, "High efficiency frequency tripling schemes for high-power Nd:glass lasers," *IEEE J. Quant. Electron.* vol. QE-17, No. 9, 1771-1782, Sept. 1981.
8. W. Seka, S. D. Jacobs, J. E. Rizzo, R. Boni, and R. S. Craxton, "Demonstration of high efficiency third harmonic conversion of high power Nd-Glass laser radiation," *Opt. Comm.*, vol. 34, pp. 469-473, Sept. 1980.
9. J. A. Armstrong, N. Bloembergen, J. Ducing, and P. S. Pershan, "Interactions between light waves in a nonlinear dielectric," *Phys. Rev.* vol. 127, pp. 1918-1939, Sept. 1962.

10. P. A. Franken and J. F. Ward, "Optical harmonics and Nonlinear Phenomena," *Rev. Mod. Physics*, vol. 35, pp. 23-39, Jan. 1963.
11. A. Szilagy, A. Hordvik, and H. Schlossberg, "A Quasi-phase-matching technique for efficient optical mixing and frequency doubling," *J. Appl. Phys.*, vol. 47, pp. 2025-2032, May 1976.
12. D. E. Thompson, J. D. McMullen, and D. B. Anderson, "Second-harmonic generation in GaAs 'stack of plates' using high-power CO₂ laser radiation," *Appl. Phys. Lett.* vol. 29, pp. 113-115, July 1976.
13. M. S. Piltch, C. D. Cantrell and R. C. Sze, "Infrared second-harmonic generation in nonbirefringent cadmium teluride," *J. Appl. Phys.*, vol. 47, pp. 3514-3517, Aug. 1976.
14. Okada, *Opt. Commun.* 18,331,1976 several quartz crystals
15. J. M. Yarborough, J. Falk, and C. B. Hitz, "Enhancement of optical second harmonic generation by utilizing the dispersion of air," *Appl. Phys. Lett.*, vol. 18, pp. 70-73, Feb. 1971.
16. V. D. Volosov, A. G. Kalintsev, and V. N. Krylov, "Suppression of degenerate parametric processes limiting frequency-doubling efficiency of crystals," *Sov. J. Quantum. Electron.*, vol. 6, pp. 1163-1167, Oct. 1976.
17. D. Eimerl, "High average power harmonic conversion," *IEEE. J. Quant. Electron.*, vol. QE-23, No. 5, 575-593, May, 1987.
18. M. A. Norton, D. Eimerl, C. A. Ebberts, S. P. Velsco, and C. S. Petty, "KD*P frequency doubler for high average power applications," *SPIE*, vol. 1223 *Solid State Lasers*, pp. 75-83, 1990.
19. C. B. Dane, L. E. Zapata, W. A. Neuman, M. A. Norton, and L. A. Hackel, "Design and operation of a 150 W near diffraction-limited laser amplifier with SBS wavefront correction," *IEEE J. Quant. Electron.*, vol. 31, pp. 148-162,
20. L. D. Siebert, N. K. Moncur, W. W. Lawrence, R. J. Masters, R. P. Johnson, and M. B. Beyers, "Multiple-crystal high-efficiency frequency conversion for long-pulse lasers," Paper THK6, CLEO, 1987, Washington D. C., *OSA Tech. Dig. Sers.*, vol. 14, pp. 258, 1987. Jan. 1995.
21. D. Eimerl, "Quadrature frequency conversion," *IEEE. J. Quant. Electron.*, vol. QE-23, No. 8, 1372-1378, Aug., 1987.

22. M. S. Pronko, R. H. Lemberg, S. Obenschain, C. J. Pawley, C. K. Manka, and R. Eckardt, "Efficient second harmonic conversion of broadband high-peak-power Nd:glass laser radiation using large-aperture KDP crystals in quadrature," *IEEE J. Quant. Electron.*, vol. 26, pp. 337-347, Feb. 1990.
23. D. Eimerl, J. M. Auerbach, D. Milam, and P. W. Milonni, "Three- and four-crystal designs for efficient third-harmonic generation," submitted to *Optics Letters*.
24. W. J. Hogan, J. A. Paisner, W. H. Lowdermilk, M. S. Sorem, J. D. Boyes, and S. A. Kumpkin, "National-Ignition-Facility design, performance and cost," *Institute of Physics Conference Series*, vol. 140, pp. 71, (London, 1995).
25. L. E. Miller, in *Handbook of Geophysics* (MacMillan, New York, 1960), pp. 13-24.
26. V. G. Dmitriev, E. A. Shalaev and E. M. Shvom, "Enhancement of the efficiency of second harmonic generation inside a resonator," *Sov. J. Quant. Elect.* vol. 4, pp. 1083-1085, Mar. 1975.
27. G. W. C. Kay and T. H. Laby, *Tables of Physical and Chemical Constants and Some Mathematical Functions*, 12th ed., Longmans, London (1959)
28. M. A. Summers and R. D. Boyd, To our knowledge, this work was never published. The results are available in "Frequency conversion-experiments and theory, a collection of conversion studies for Nova."
29. S. P. Velsco and D. Eimerl, "Precise measurements of optical dispersion using a new interferometric technique," *Appl. Opt.*, vol. 25, No. 8, 1344-1349, April 1986.

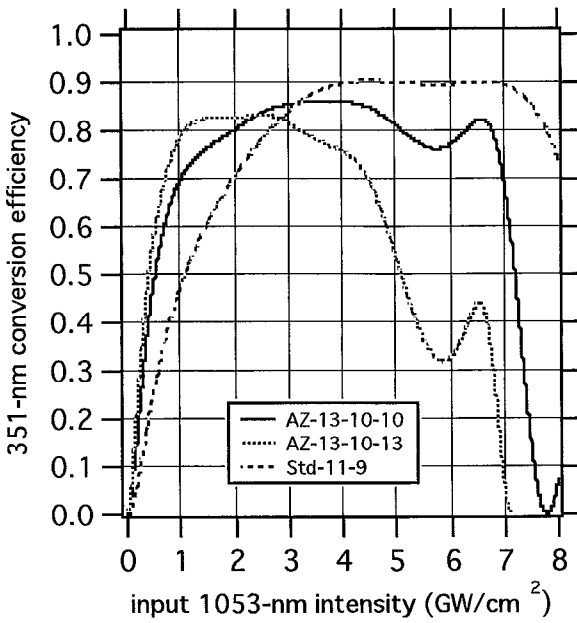


Fig. 1. Comparison of the conversion curves for two optimized alternating-Z triplers and one standard two-crystal. Numerals in the legend are crystal thicknesses in mm.

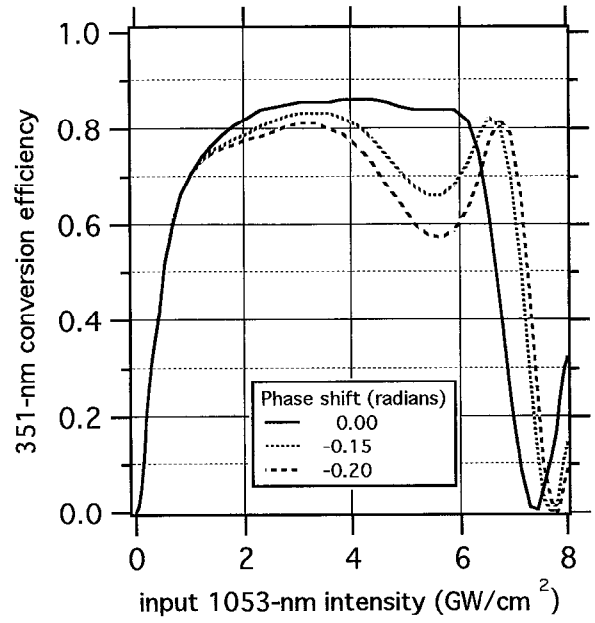


Fig. 2. Effect on conversion efficiency of phase lag of the 527-nm wave due to dispersion in the air gap between the doublers in an alternating_Z tripler.

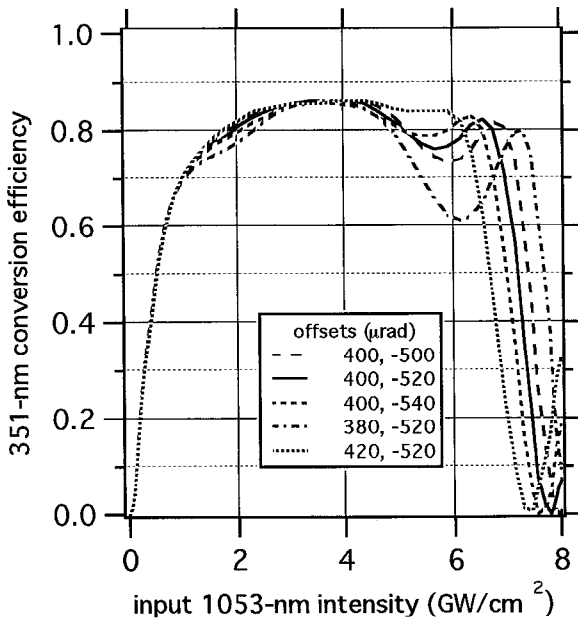


Fig. 3. Effect of small errors in angular offsets of the doublers in an AZ-13,10,10 tripler.

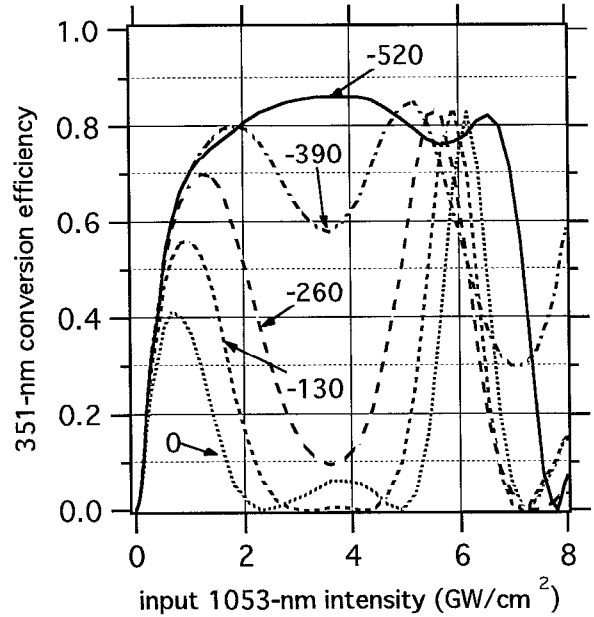


Fig. 4. Effect of large errors in the angular offset of the 10-mm doubler in an AZ-13-10-10 tripler. Offset of 13-mm doubler was +400 mrad for all cases.

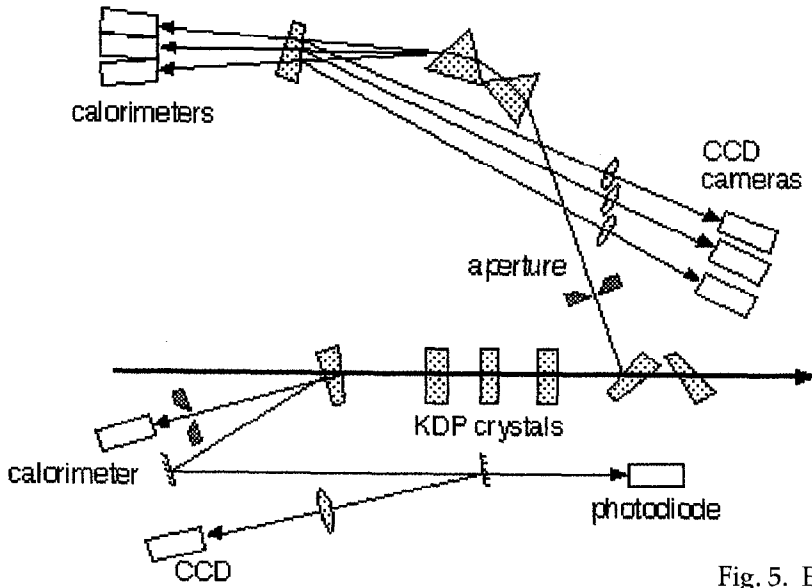


Fig. 5. Experimental arrangement for measuring conversion efficiency.

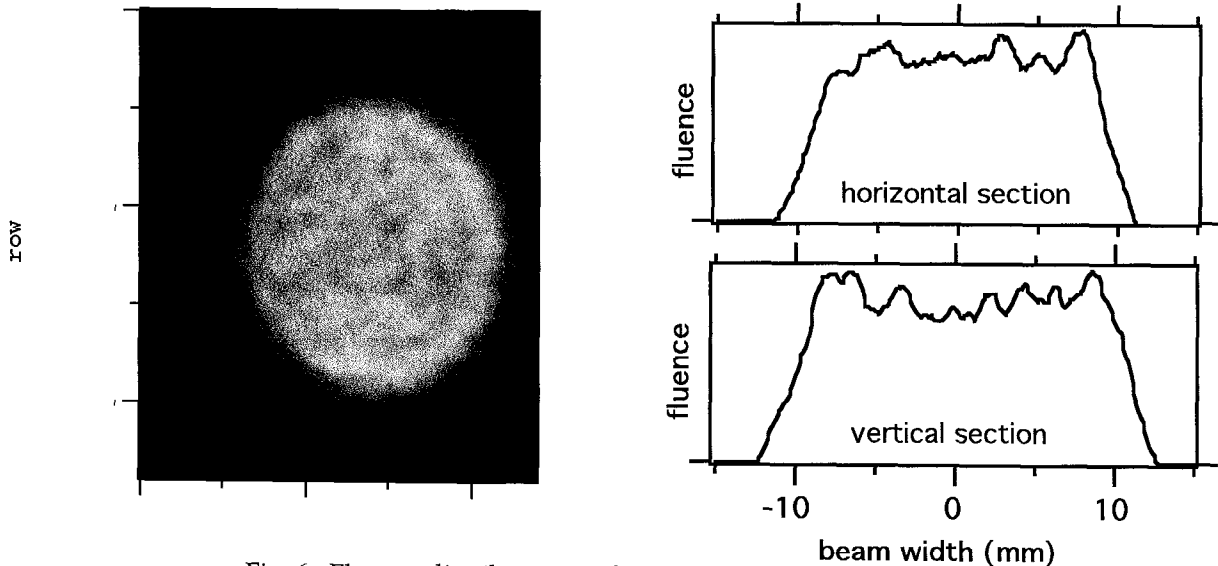


Fig. 6. Fluence distribution in the input 1053-nm beam.

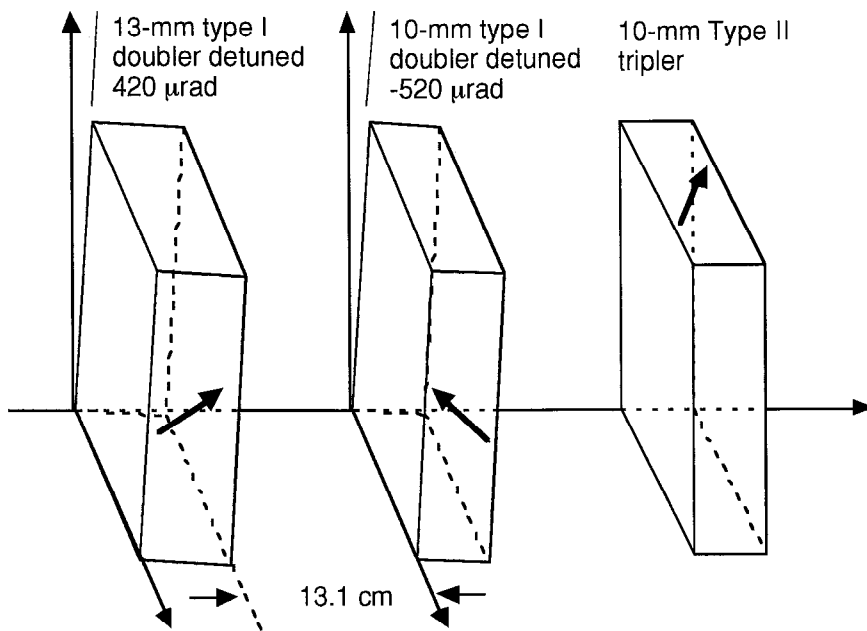


Fig. 7. Arrangement of the converter crystals

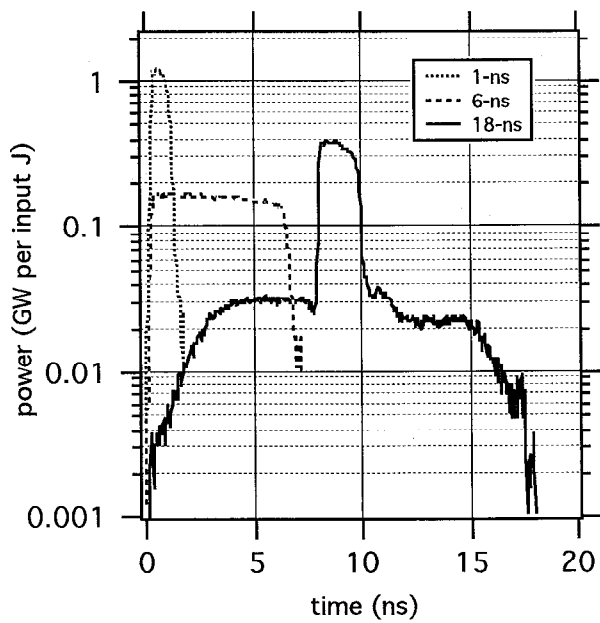


Fig.8. Waveforms of the input 1053-nm pulses.

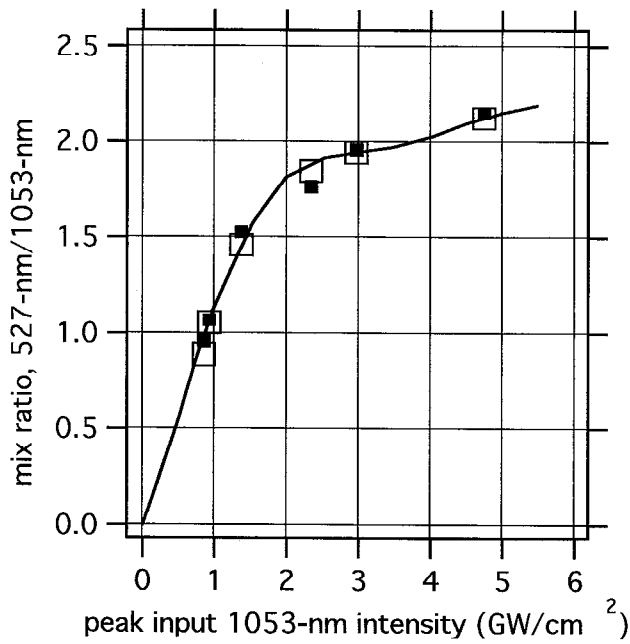


Fig. 9. Mix ratio. Solid symbols--measured with 6-ns pulses. Open symbols--calculated shot by shot. Curve--calculated assuming all waveforms identical.

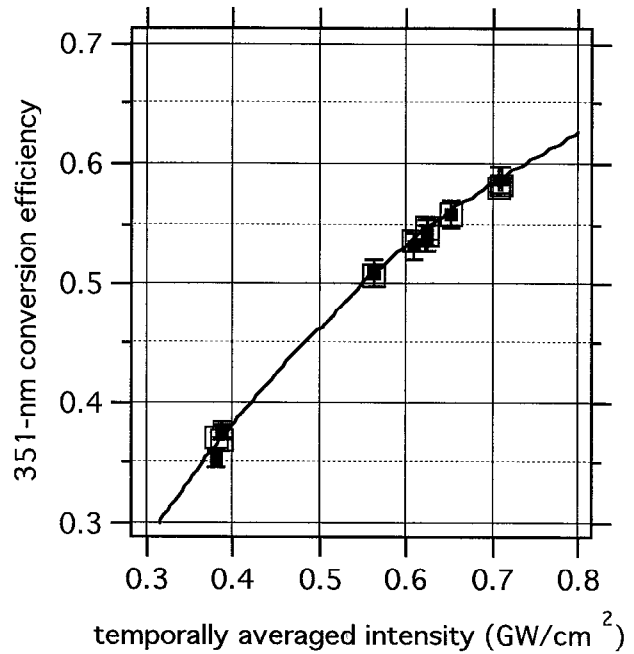


Fig. 10. Conversion efficiency. Solid symbols--measured with 6-ns pulses. Open symbols--calculated shot by shot. Curve--calculated for rectangular waveform.

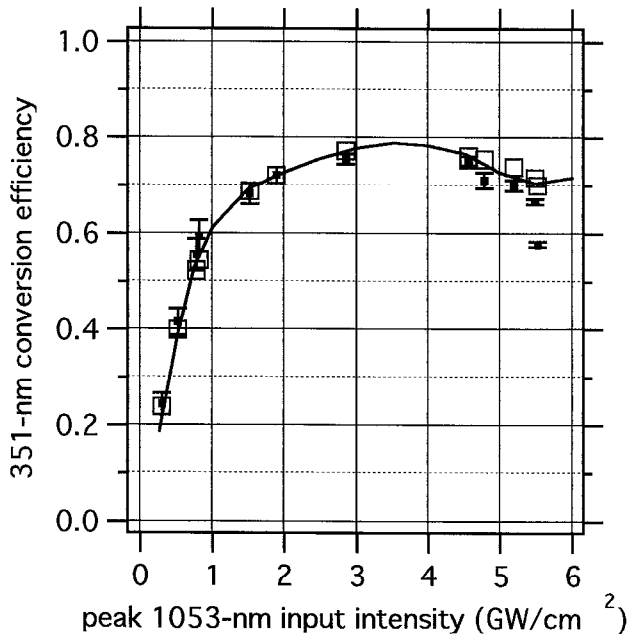


Fig. 11. 1053nm to 351-nm conversion efficiency. Solid symbols--measured with 1-ns pulses. Open--calculated shot by shot. Curve--calculated assuming that all pulses had identical waveforms.

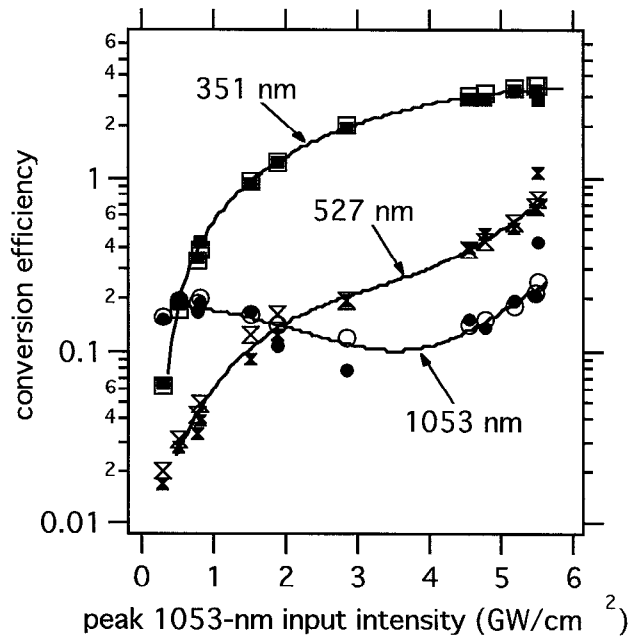


Fig. 12. Output fluence at all three harmonics for the 1-ns conversion experiment. Solid and open symbols denote measurements and shot by shot calculations. Curves are empirical fits to all data, either measured or calculated.

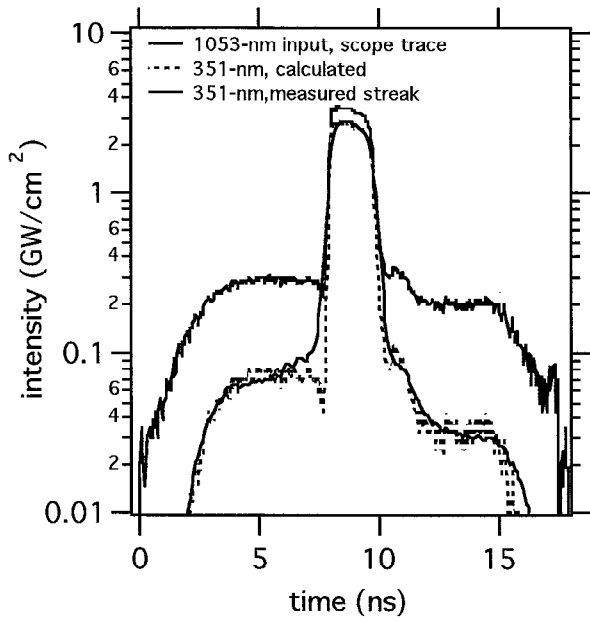


Fig. 13. Conversion of a pulse with with peak intensity of 3.4 GW/cm^2 and intensity ratio of 12:1 to produce a 351-nm pulse with peak intensity of 2.8 GW/cm^2 and intensity ratio of 42:1.

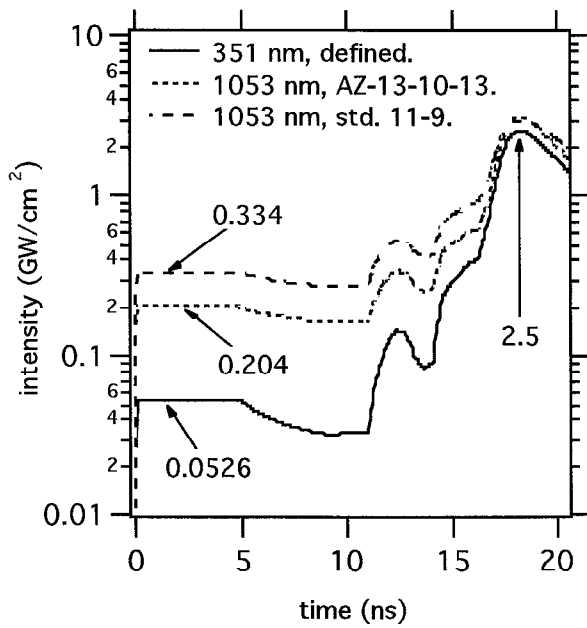


Fig. 14. A NIF 21-ns 351-nm pulse, and the input 1053-nm pulses that are required if the tripler is either an AZ-13-10-13 or a standard 11-9.

Table 1. An optimized design for an alternating-Z tripler.
 Units are μrad , GW/cm^2 , and mm.

Type I/Type I/Type II, Alternating-Z	Optimum
Beam polarization	90°
Beam divergence	30-50
Intensity minimum	0.01
Intensity maximum	6
First doubler length	13
First doubler offset	400
Second doubler length	10
Second doubler offset	-520
Air path phase error	0
Mixer length	13
Mixer offset	0
Crystal deuteration level	80%

Table 2. Transmittances of the 6 surfaces in the tripler.

wavelength	input	all 4 interior surfaces	output
1053 nm	0.999	0.991	0.976
527	0.961	0.984	0.988
351	0.996	0.957	0.972

Table 3. Data for conversion of shaped pulses. Intensities are in GW/cm².

Shot	1906	1907
Peak 1053-nm intensity	3.44	3.04
Peak 351-nm intensity, measured	2.82	2.45
Peak 351-nm intensity, calculated	2.86	2.52
351-nm intensity ratio, measured	42:1	48:1
351-nm intensity ratio, calculated	36:1	46:1
energy conversion, measured	62%	59%
energy conversion, calculated	62%	59%
peak conversion, measured	82%	81%
peak conversion, calculated	83	83%

Table 4. Comparison of the merit of four triplers in the generation of a 21-ns, 351-nm laser pulse with 50:1 intensity variation. Edge and peak intensities are identified in Fig. 16. Conversion efficiencies were calculated.

tripler	1053-nm intensity		conversion efficiency	
	leading-edge	peak	energy	peak
AZ-13-10-13	0.204	3.08	68%	81%
AZ-13-10-10	0.235	2.93	65	85
AZ-13-10-10(ph. error)	0.253	3.12	62	80
std. 11-9	0.334	2.98	55	84